AN ACTIVE TISSUE-CONTRAST SENSING MICROSYSTEM FOR BIOPSY NEEDLES: INITIAL RESULTS

Tao Li[*] and Yogesh B. Gianchandani
Engineering Research Center for Wireless Integrated Microsystems
University of Michigan, Ann Arbor, MI, USA

ABSTRACT

This paper describes progress toward an active tissue-contrast sensing microsystem that can be embedded at the tip of a fine biopsy needle. An analog CMOS chip is integrated with a piezoelectric sensor to reduce the impact of parasitic capacitances and allow differential sensing that will permit deep tissue sampling. The sensor element and the CMOS circuit are fabricated in-house and integrated onto the tip of a 20-gauge needle. The sensor module with integrated interface circuit has a size of 950 μm (L) × 350 μm (W) × 220 μm (H). It can successfully generate an oscillating signal as the readout of the integrated piezoelectric quartz sensor. Preliminary functional verification for sensing is provided by saline solutions of 0.5-3% concentration, representing a progressive increase of acoustic impedance. As expected the measured frequency shifts increase with higher saline concentration, indicating the validity of the sensor interface circuit design.

INTRODUCTION

Fine needle aspiration (FNA) biopsy is a common clinical procedure for harvesting cells from the thyroid, breast, etc. for subsequent cytological examination [1]. It is typically performed with 20-27 gauge needles, with outer diameter <1 mm, and is challenging in itself due to the precision required in acquiring the desired sample from the small target volumes. Real-time ultrasound imaging provides only a partial solution despite the added complexity. For example, even with such imaging, at least 2-5% of thyroid FNAs are read as non-diagnostic because of improper sampling [2-4].

We have previously reported a passive sensor element for detecting tissue contrast during FNA biopsy of thyroid nodules [5]. It used a micromachined piezoelectric sensor integrated into a cavity at the tip of a biopsy needle to distinguish tissue planes in real time by measuring the electrical impedance spectra of the sensor with an impedance analyzer. The frequency and magnitude of an impedance resonance peak showed tissue-specific characteristics as the needle was inserted into testing tissue, and a proportional relationship between the frequency shift and sample acoustic impedance was found. A single wire located within the lumen supplied power to the sensor element; the wall of the needle served as the ground terminal. However, signal attenuation and stray capacitances caused by the needle tube and surrounding tissue can become substantial in certain tissue environments or at large insertion depth. The passive sensor cannot effectively differentiate tissue contrast when the needle penetration depth is greater than ≈15 mm, limiting its application in actual biopsy procedures, particularly for deep tissue.

This paper describes an active tissue-contrast sensing microsystem that can be embedded at the tip of a fine biopsy needle. An analog CMOS chip is integrated with a piezoelectric sensor to address the issues encountered with the passive device, and to eliminate the requirement of readout equipment such as the impedance analyzer so that this technology can be potentially low-cost and widely accessible. The sensor element and CMOS circuit are fabricated in-house and integrated onto the tip of a 20-gauge biopsy needle. Preliminary measurement results for functional verification are reported.

DEVICE CONCEPT

As shown in the system scheme diagram (Fig. 1), an active sensor chip with interface circuit is integrated at the tip of a biopsy needle to provide tissue contrast detection for guidance of needle tip positioning. The sensor is made from a bulk piezoelectric quartz crystal or alternatively, high-Q lead zirconate titanate (PZT). The interface circuit establishes a resonant oscillation that permits the piezoelectric sensor to be read out locally with diminished dependence on parasitic capacitances. This oscillation signal is then transmitted to an external unit by an intra-luminal wire for readout and display. Two additional wires provide the power and ground in this scheme.
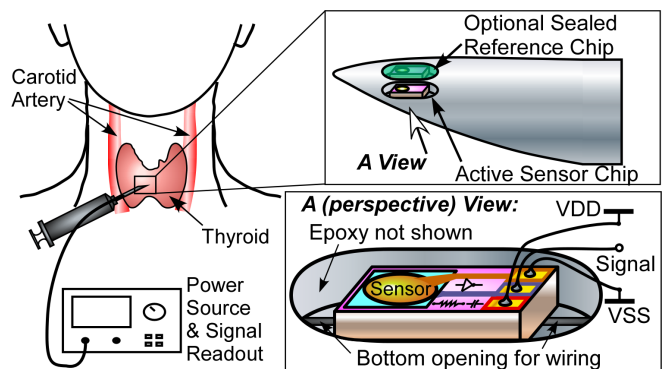

Fig. 1: System diagram of the piezoelectric sensor with integrated interface circuit intended for in-situ tissue contrast detection during an FNA biopsy.

[*] *Corresponding author:* 1301 Beal Ave., Ann Arbor, MI, 48109, USA; Tel: 1-734-615-7983, Fax: 1-734-763-9324, Email: litz@umich.edu
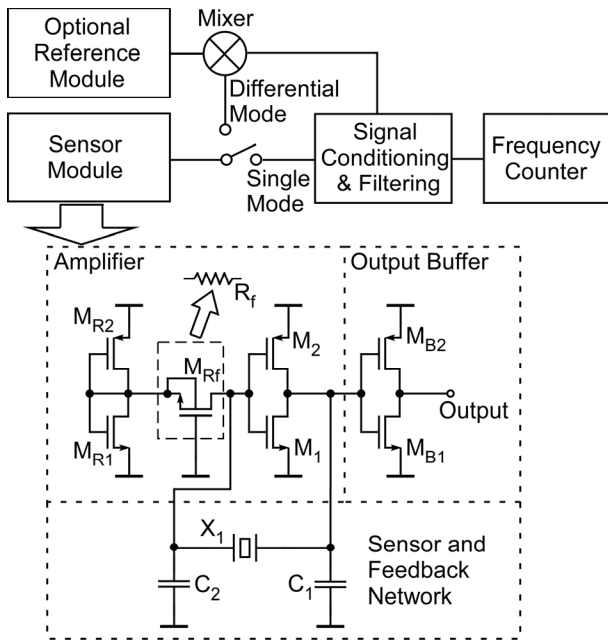
Fig. 2: Block diagram and implementation of the interface circuit for the piezoelectric sensor for single-mode or optional differential-mode operations.

The signal conversion provided by the interface circuit also enables optional differential-mode operation of the sensor for further reduction of common-mode parasitic capacitances and other interferences from the human body. This can be done by integrating an additional reference module sealed in acoustically-insulating material, such as epoxy, beside the active sensor chip, and then subtracting the output signals of their interface circuits.

The dimensions of the sensor chip are limited by the size of the cavity that can be made on the sidewall of the needle tube, and a chip size (before sensor integration) of 950 μm (L) × 350 μm (W) × 100 μm (H) is selected for a 20-gauge needle.

The commonly-used Pierce oscillator circuit has been modified as shown in the lower part of Fig. 2, enabling easy implementation using CMOS process, in a single chip with limited available area. This circuit is used as the interface circuit for resonance frequency readout from the piezoelectric sensor. In the circuit, an inverter is used as a high-gain and high-bandwidth amplifier that provides a phase shift of approximately 180°. The feedback network formed by the sensor X_1 and R_1, C_1, and C_2 provides another 180° phase shift at its resonance frequency, making the total phase shift around the loop to be 360° and satisfying one of the Barkhausen criteria required to sustain oscillation. The other condition requires a closed-loop gain ≥1 for startup and sustaining oscillation, and can be provided with proper design of the amplifier gain and values of the feedback network elements. In the new biasing method for the amplifier, a biasing voltage that sets the inverter in the high-gain linear region is generated using a reference inverter consisting of two diode-connected transistors (M_{R1} and M_{R2})

with the same dimensions as M_1 and M_2, respectively. This biasing voltage is then transferred to the amplifying inverter through R_f. The input impedance of this configuration is $Z_{in} \approx R_f$; it reduces the required value of R_f by a ratio of the amplifier open loop gain A. As R_f is only connected to the input node of the amplifying inverter, it is not subject to the large signal variations present at the output node of the amplifier, making it easier to implement this resistor with special techniques such as the active NMOS resistor M_{Rf} shown in Fig. 2. The feedback capacitors C_1 and C_2 are made as pseudo-variable capacitors and can be trimmed by laser.

The output signals from the interface circuits of the active and optional reference sensors can be fed into an external mixer followed by a low pass filter to obtain the frequency difference (differential readout), which can be picked-up by a frequency counter and subjected to further data analysis.

DEVICE FABRICATION

The single-chip sensing microsystem is fabricated with a 12-mask process (Fig. 3). The interface circuit is formed using the in-house University of Michigan 3 μm p-well CMOS process in the n-epi layer on a p-type silicon wafer. Post-CMOS processing is then performed to make recesses and metal electrodes for sensor integration. The sensor can be batch-fabricated from quartz crystal or high-Q PZT using a customized process, in which batch-mode micro-electro-discharge-machining (μEDM) is used to form a steel tool that is subsequently used for batch-mode micro ultrasonic machining (μUSM) [6,7]. Dicing can be used for rapid prototyping of square geometries. After wafer thin-down and chip release, the sensor is integrated onto the chip, followed by parylene encapsulation.

Figure 4 shows a circuit die photograph. The area of the interface circuit is 600×270 μm^2, including all transistors, trimmable / regular capacitors, active / passive resistors, protective diodes for electrostatics and metal pads for wire bonding and probing. Figure 5(a) shows the square
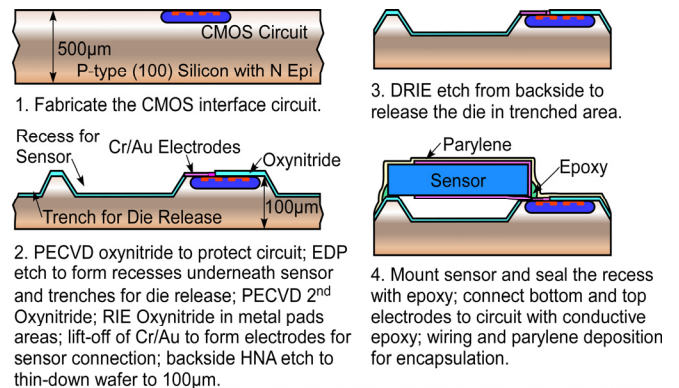

1. Fabricate the CMOS interface circuit.

3. DRIE etch from backside to release the die in trenched area.

2. PECVD oxynitride to protect circuit; EDP etch to form recesses underneath sensor and trenches for die release; PECVD 2nd Oxynitride; RIE Oxynitride in metal pads areas; lift-off of Cr/Au to form electrodes for sensor connection; backside HNA etch to thin-down wafer to 100μm.

4. Mount sensor and seal the recess with epoxy; connect bottom and top electrodes to circuit with conductive epoxy; wiring and parylene deposition for encapsulation.

Fig. 3: Fabrication process flow for the single-chip sensing microsystem. In-house 3 μm CMOS process at the University of Michigan is used for the circuit fabrication, but any other CMOS process will also be adequate.
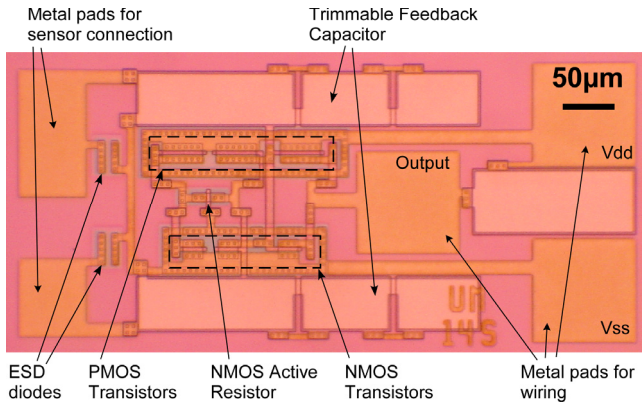
Fig. 4: A microscopic die shot of one type of the fabricated circuit chips with a reference inverter and an active feedback resistor, before post-CMOS processing is carried out. The die area is $600 \times 270 \ \mu m^2$.

quartz sensors fabricated by dicing an AT-cut single crystal quartz disc with patterned Ti/Au electrodes on the top and bottom surfaces. Epoxy is used to mount the quartz disc during dicing for adequate bonding strength between the small diced chip and the glass carrier substrate. The lateral dimensions of the square quartz sensor are $300 \times 300 \ \mu m^2$, and the thickness can vary between 80 μm and 200 μm for different target resonance frequencies. Figure 5(b) shows a sensor module with a square quartz sensor integrated on an interface circuit chip, mounted on a glass carrier substrate for testing purpose. The size of the sensor module is 950 μm (L) × 350 μm (W) × 220 μm (H). The lead transfer
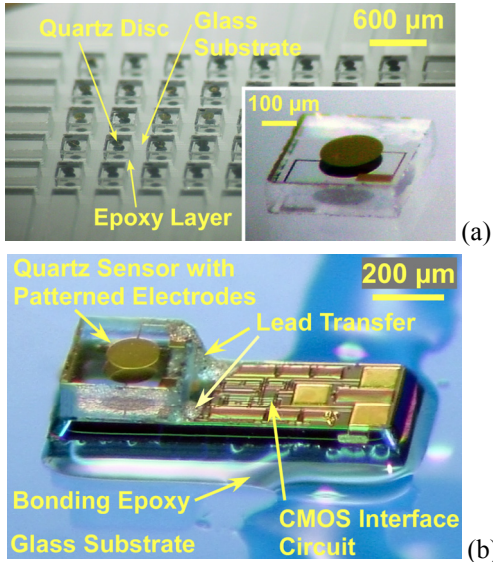

Fig. 5: Photos of: (a) an AT-cut quartz substrate diced for patterns of quartz square plates, with the insert showing a released quartz square sensor with patterned Ti/Au electrodes on top and bottom surfaces; (b) an active sensing module with quartz sensor integrated on the CMOS interface circuit chip, mounted on a glass substrate for testing purpose. Size of the sensor module: 950 μm (L) × 350 μm (W) × 220 μm (H).
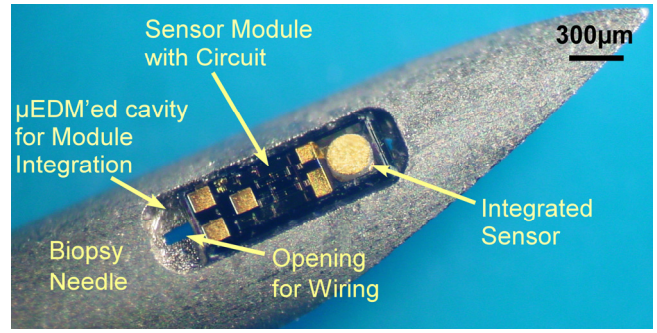

Fig. 6: Photo of an active module with an integrated sensor and interface circuit incorporated into the tip of a 20-gauge biopsy needle (outer diameter <1 mm), before wiring and sealing with epoxy. Size of the module: 950 μm (L) × 350 μm (W) × 150 μm (H).

from the electrodes on the quartz sensor to the circuit chip is made by using conductive epoxy for this preliminary proof of concept. Figure 6 shows a sensor module incorporated into the tip of a 20-gauge biopsy needle, before wiring and epoxy-sealing. The cavity on the biopsy needle is formed by μEDM with a size of 1400 μm (L) × 400 μm (W) × 100 μm (D), leaving an opening for wiring at the center bottom of the cavity due to the tubular geometry of the needle. An additional cavity can be formed on the needle in the same way for the optional reference sensor module. The integrated disc sensor shown in the figure is batch-fabricated from PZT by the customized μUSM process, with a diameter of 200 μm and a thickness of 50 μm. The size of the sensor module is 950 μm (L) × 350 μm (W) × 150 μm (H), with the smaller height due to a thinner sensor.

MEASUREMENT RESULTS

The analog CMOS interface circuit was tested for process evaluation and Table I presents the measurement results of selected CMOS process parameters. Due to the robustness of the circuit configuration, deviation in the thresholds and *KP* of the fabricated CMOS transistors from the design targets did not affect the operation of the circuit. The amplifier in the circuit was also tested in the open loop without connecting the sensor X_1 and the results for selected

Table I: Measurement results of selected CMOS process parameters and interface circuit performance.

CMOS threshold [V]	-0.934 / 0.967 (PMOS/NMOS)
KP [μA/V²]	17.22 / 47.51 (PMOS/NMOS)
Poly1/Poly2 capacitance [fF/μm²]	0.470
Passive Feedback Resistor R_f [KΩ]	11.00
Values of C_1/C_2 after laser trimming [pF]	3.40 / 3.40
Power supply V_{DD}-V_{SS} [V]	10
Voltage gain@1KHz [V/V]	≈392
-3 dB bandwidth [MHz]	1.56
Amplifier gain at 3 dB bandwidth [V/V]	≈278

performance parameters are listed in Table I. A voltage gain of ≈392 at 1 KHz and a 3 dB bandwidth of 1.56 MHz were obtained.

The integrated active quartz-sensor module shown in Fig. 5(b) was tested on a probe station. With a power supply of 10 V, an oscillation signal at ≈26.2 MHz was successfully generated at the output signal path as the sensor readout. This frequency is close to the frequency at the third harmonic mode (30 MHz) of the original quartz disc. The reason is still under investigation and possibly related to the loading effects to the sensor from the chip substrate and lead transfer.

Preliminary functional verification for sensing is provided by saline solutions using the fabricated CMOS chip and a quartz crystal sensor disk (Φ8.64 mm) of 5 MHz resonant frequency, which provides convenience for sample loading and testing. Figure 7 shows measured frequency shifts (on the left axis) in tests with saline solutions of 0.5-3% concentration, which represent a progressive increase of acoustic impedance as indicated by the straight line to the right axis. The frequency shifts increase with higher saline concentration, as expected, indicating the validity of the sensor interface circuit design.

CONCLUSIONS

An active tissue-contrast sensing microsystem that can be embedded at the tip of a fine biopsy needle has been investigated. An analog CMOS chip was integrated with a piezoelectric sensor to address the issues encountered with the passive device and to eliminate the requirement of expensive readout equipment. The in-house fabricated sensor module with integrated interface successfully generated an oscillating signal as the readout of the piezoelectric quartz sensor. Functional verification for sensing was provided by the use of saline solutions. The measured frequency shifts increase with higher saline concentration, validating the sensor interface circuit design and the feasibility of the design concept. Future effort will be directed to further testing and performance evaluation of the microsystem, as well as tissue loading measurements in single and differential mode operation.

ACKNOWLEDGEMENT

Fig. 7: *Measured oscillation frequency shift in preliminary tests with saline solutions of concentration between 0.5% and 3%. As shown in the curve to the right axis [8], a higher saline concentration results in a higher acoustic impedance, which, in turn, is indicative of density. A quartz crystal sensor disk (Φ8.64 mm) with 5 MHz resonance frequency, and droplet volumes of 0.3 μL are used with the fabricated interface circuit for this preliminary test.*

REFERENCES

[1] J. T. Johnson and L. Zimmer, *Fine-Needle Aspiration of Neck Masses*, eMedicine World Medical Library from WebMD, 2005, www.emedicine.com/ent/topic561.htm.
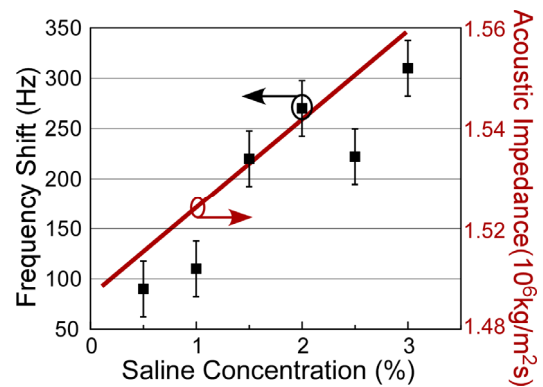
[2] F. Pacini and L.J. De Groot, "Thyroid Neoplasia," *The Thyroid and its Diseases*, 6th ed., W.B. Saunders Company, 1996, updated online at www.thyroidmanager.org, May 2004.

[3] S. Takashima, H. Fukuda, and T. Kobayashi, "Thyroid nodules: clinical effect of ultrasound-guided fine-needle aspiration biopsy," *J. Clin. Ultrasound*, 22(9), pp. 535-42, Nov.-Dec. 1994.

[4] H. Gharib and J.R. Goellner, "Fine-needle aspiration biopsy of the thyroid: an appraisal," *Ann. Intern. Med.*, 118(4), pp. 282-9, Feb. 1993.

[5] T. Li, R. Y. Gianchandani, and Y. B. Gianchandani, "Micromachined bulk PZT tissue contrast sensor for fine needle aspiration biopsy," *Lab on a Chip*, vol. 7, no. 2, pp. 179-185, Feb. 2007.

[6] T. Li and Y. B. Gianchandani, "A micromachining process for die-scale pattern transfer in ceramics and its application to bulk piezoelectric actuators," *IEEE/ASME J. Micromechanical System*, vol. 15, no. 3, pp. 605-612, Jun. 2006.

[7] T. Li and Y. B. Gianchandani, "A high speed batch mode ultrasonic machining technology for multi-level quartz crystal microstructures," *IEEE International Conference on Micro Electro Mechanical Systems*, Hong Kong, pp. 398–401, 2010.

[8] F.T. Gucker, C.L. Chernick, and P. Roy-Chowdhury, "A frequency-modulated ultrasonic interferometer: adiabatic compressibility of aqueous solutions of NaCl and KCl at 25°C," *Chemistry*, vol. 55, pp. 12-19, 1966